Use of Natural Rubber Prophylactics Waste as a Potential Filler in Styrene–Butadiene Rubber Compounds

GEORGE MATHEW,[1] R. P. SINGH,[2] R. LAKSHMINARAYANAN,[3] and SABU THOMAS[1,*]

[1]School of Chemical Sciences, Mahatma Gandhi University, Priyadarshini Hills P.O., Kottayam 686 560, Kerala, [2]Polymer Chemistry Division, National Chemical Lab, Pune, and [3]Elastomer Technical Services, Pudur, Madurai, India

SYNOPSIS

Owing to the unstable nature of the latex compound and the strict specifications in the quality of latex products such as condoms and examination gloves, the rejection in the latex industry comes to about 10 to 15% of the rubber consumed. These latex rejects contain about 95% rubber hydrocarbon of very high quality. A cost-effective technique has been developed for the reuse of natural rubber (NR) prophylactics waste in styrene–butadiene rubber (SBR). The influence of powdered latex rejects on the curing characteristics, mechanical properties, and failure behavior of SBR has been investigated. More emphasis is placed on the effect of both particle size and the loading of latex waste filler. Swelling studies were carried out to establish the degree of crosslinking of SBR and to assess the extent of interaction between the matrix and latex waste filler of varying particle sizes. A three layer model has been set up to study the diffusion of sulfur from the matrix phase to the filler phase. Scanning electron microscopy has been used to analyze the particle morphology, filler dispersion, and filler–matrix interface adhesion. The results of the study revealed that NR prophylactics rejects can be used effectively as a potential filler in SBR up to about 40 phr loading. © 1996 John Wiley & Sons, Inc.

INTRODUCTION

In recent years, there has been a great deal of interest in polymer industry about the development of cost effective techniques to convert waste and used rubber in to a processable form.[1-6] Many efforts have been made to lower rubber compound cost and to conserve raw materials and energy by the use of reclaimed rubber. Researchers have used various techniques, such as chemical,[1,7] thermomechanical,[3,6] and cryomechanical[2,4,8,9] processes. Even though the use of reclaimed rubber claims economic advantages, it constitutes only a small percentage of the raw rubber consumption because of its inferior physical properties.

Compared to reclaimed rubber, scrap latex rejects have recently become a focus of attention because of the lightly crosslinked and the high quality nature of the rubber hydrocarbon. As a result of the unstable nature of the latex compound and the strict specifications in the quality of latex products such as condoms and gloves, the rejection in the latex industry comes to about 10% to 15% of the rubber consumed. The reuse of natural rubber latex waste is not only a matter of economy but a matter of ecology also because natural rubber takes several decades to decompose. Discarded prophylactics, which are rich in rubber hydrocarbon, should be returned to the production cycle as long as latex industries are faced with the problem of disposal. The papers published in this broad field of recycling may be generally divided into the following areas.

- Studies on the various recycling techniques.[1,7]
- Methods of characterization of rubbercrumbs.[10-13]
- Studies on the interface of rubber crumbs/polymer matrix.[14,15]
- Influence of shape, size, and loading of crumb particles on the properties.[16-18]

* To whom correspondence should be addressed.

Journal of Applied Polymer Science, Vol. 61, 2035–2050 (1996)
 CCC 0021-8995/96/112035-16

- Effect of chemical modification of rubber crumbs.[17-19]

In addition to these, Acetta and Vergnaud[20,21] tried to upgrade scrap rubber powder by vulcanization without new rubber. Phadke et al.[22,23] studied the mechanical properties and rheological behavior of cryoground rubber–natural rubber blends. Sharapova et al.[24] investigated the role of sulfur diffusion in the vulcanization of rubbers containing comminuted scrap using a three layer model. Onouchi et al.[25] reclaimed crushed tire scrap with dimethyl sulfoxide. The Rubber Research Institute of India[26] and the Rubber Research Institute of Malaysia[27,28] have independently developed a technique for reclaiming latex rejects. However, more in-depth studies on the influence of particle size and loading of latex waste filler in rubber compounds are lacking. In this paper, we report on an economic method to convert latex rejects to a processable form and to reuse them as a filler in styrene butadiene rubber. Emphasis has been given to understand the influence of both particle size and loading of filler on the curing characteristics and mechanical performance of the vulcanizates. Swelling studies were carried out to understand the interaction of the latex waste filler with the SBR matrix. Sulfur diffusion in these compounds has been analyzed by the help of a three layer model. Particle morphology, filler dispersion, and filler–matrix interface adhesion were analyzed using scanning electron microscopy (SEM).

EXPERIMENTAL

Materials

Styrene–butadiene rubber (SBR; Synaprene 1502) was supplied by Synthetics and Chemicals Ltd, Bhitaura, Bareilly, UP, India. Styrene Content was 25.5%. NR latex waste filler was prepared from waste latex condom rejects supplied by Hindustan Latex Ltd., Thiruvananthapuram, Kerala, India. Rubber additives were as follows: zinc oxide, stearic acid, *N*-cyclohexylbenzthiazyl sulphenamide (CBS), trimethyl dihydroquinolin (TDQ), and sulfur (all are commercial grades). A reagent grade of toluene was also used.

Preparation and Characterization of Powder Rubber

Our size reduction system for powdering NR latex waste doesn't involve any expensive machinery. The size reduction was carried out by a mechanical grinding process in a fast rotating toothed wheel mill to get a polydispersed rubber powder. The powder was separated into three different particle sizes, with size increases in the following order: size 1 (S1) < size 2 (S2) < size 3 (S3).

We have prepared size 4 filler by passing the latex waste through a hot two-roll mixing mill for a fixed time (5 min). The particle size reduction in this technique is very much lower than the first technique; hence, we got comparatively larger particles of sizes ranging from 5–15 mm. Each set of these sizes were characterized for particle size distribution, most frequent size range, average size, and specific gravity. Particle size distribution analysis was done using an optical microscope. A mill sheeted form (M) of the latex rejects also were prepared by passing the rejects through a two-roll mixing mill for 10 min.

Compounding

Compounding of SBR and NR prophylactics filler was done on a two-roll mixing mill (friction ratio 1 : 1.4), according to ASTM D 15-627. The basic formulation used is given in Table I. We have analyzed the effect of adding up to 40 phr of rubber powder of varying sizes, as well as the mill sheeted form, into SBR.

Sample Preparation and Testing

Uncured rubber compound was characterized by determining the optimum cure time, scorch time, and induction time using a Monsanto Rheometer, R_{100}. The cure reaction rate constant was calculated from the cure curves, and, thus, the kinetics of vulcanization also was studied. The Wallace plasticity of the rubber compounds was determined using a Wallace rapid plastimeter.

Curing of the rubber compounds was carried out in an electrically heated hydraulic press at 150°C. Dumbbell shaped tensile and angular tear specimens

Table I Basic Formulation

Material	Loading (phr)
SBR	100
Zinc oxide	5
Stearic acid	2
CBS	1
TDQ	1
Sulfur	2.2
Filler	Variable

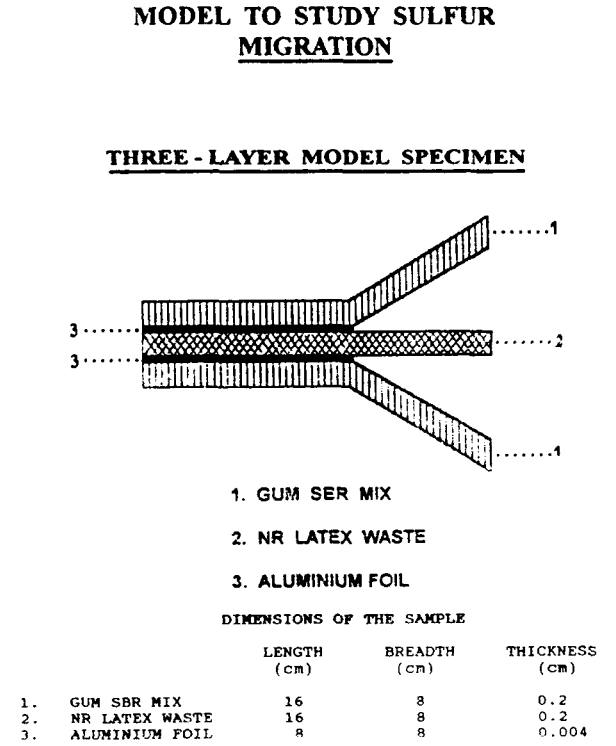

Figure 1 Model to study sulfur migration.

were punched out from the compression molded sheets along the mill grain direction. The tensile properties and the tear resistance of the compounds were measured on an Instron Universal Tensile tester, at a crosshead speed of 500 mm/min, as per ASTM D 412-80 and ASTM D 624-81, respectively. Hardness (IRHD) of the cured sheets was also tested.

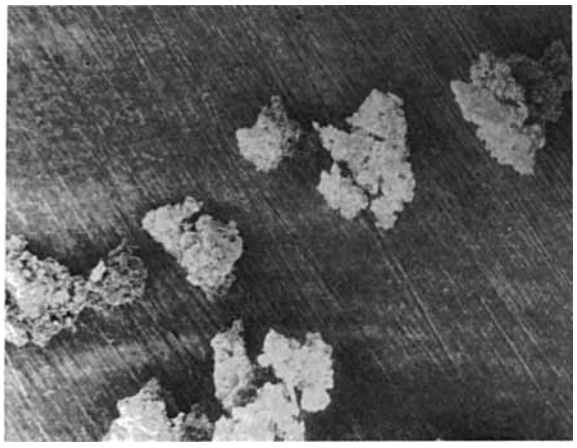

Figure 2 SEM photograph of latex waste filler particles (size 1; magnification ×60).

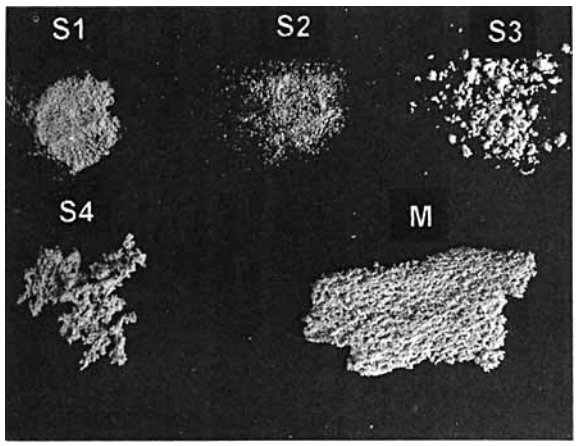

Figure 3 Photograph of varying particle sizes and mill sheeted form of latex waste filler.

Swelling Studies

To assess the swelling resistance of gum and filled SBR vulcanizates, swelling index values were determined. Circular samples of 2 cm diameter were allowed to swell in toluene at room temperature (28°C) for 72 h. The variation of crosslink density with increasing filler loading also was analyzed using swelling experiments. The equation of Kraus,[29] as well as the Cunneen and Russell equations[30] were used to assess the reinforcement of SBR matrix by latex waste filler of varying particle sizes.

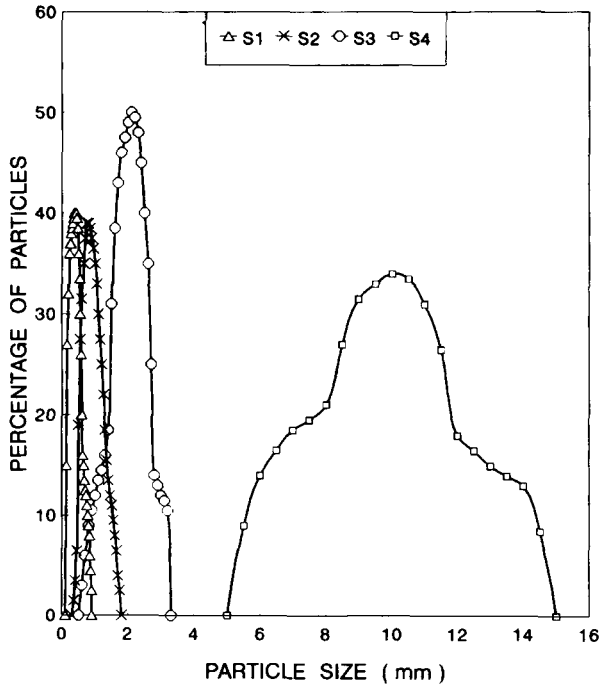

Figure 4 Particle size distribution curves.

Table II Particle Size Data

Particle Size	Most Frequent Size Range (m^2)	Average Size (m^2)
Size 1 (S1)	0.3–0.5	0.5
Size 2 (S2)	0.6–0.9	1.05
Size 3 (S3)	1.7–2.5	1.9
Size 4 (S4)	9–11	10

Sulfur Diffusion Studies

A three-layer model[24] as shown in Figure 1 was set up to study the diffusion of sulfur from the matrix phase to the filler phase. A layer of NR latex waste (containing 80 phr of size 1 filler) was sandwiched between two layers of gum SBR compounds. Size 1 filler was selected because of higher sulfur diffusion rate due to increased contact surface area with SBR matrix. In one half of the specimen, the layers of the gum SBR and latex waste were separated by an aluminium foil; in the other half, the foil was not placed. The region of the latex waste layer with the aluminium foil that will be out of contact with the two outer gum SBR layers is named as the "area not in contact"; the region of the latex waste layer without aluminium foil that will be in contact with the two outer gum SBR layers is named as the "area in contact". The system was then subjected to vulcanization at low pressure. The middle layer was separated, and the swelling index, as well as the crosslink density values were determined, by cutting circular samples from (1) the area in contact with outer gum SBR layers (denoted by CS) and (2) the area not in contact with outer gum SBR layers (denoted by NCS).

Morphology and Fractography

Morphology, filler distribution, and fractography were done using a JEOL JSM 35 C model scanning electron microscope. After tensile and tear testing, the fractured surface was carefully cut out from the failed specimen. The samples were stored in a desicator to avoid contamination and then sputter coated with gold within 24 h prior to the examination through SEM.

RESULTS AND DISCUSSION

Physical Characteristics of Ground Latex Waste

Particle Morphology

Figure 2 represents the SEM of the NR prophylactics filler particles (size 1) used in the present work. The particles are irregularly shaped with rough surface.

Particle Size Distribution

The photograph of the latex waste filler of different particle sizes and the mill sheeted form used in this study is presented in Figure 3. It is clear from the photograph that as we move from size 1 to size 4, particle size increases. Since it is possible for particles with somewhat large diameters to also penetrate the meshes due to their elasticity, it is better to represent them by size distribution curves, as given in Figure 4. Size 4 shows the most broad distribution. Size 1 and size 2 have narrow distribution, while size 3 takes the intermediate position. The most frequent size range and average particle sizes are presented in Table II. Both these values exhibit an increase as we move from size 1 to size 4. The specific gravity of the latex waste filler is determined to be 1.1529.

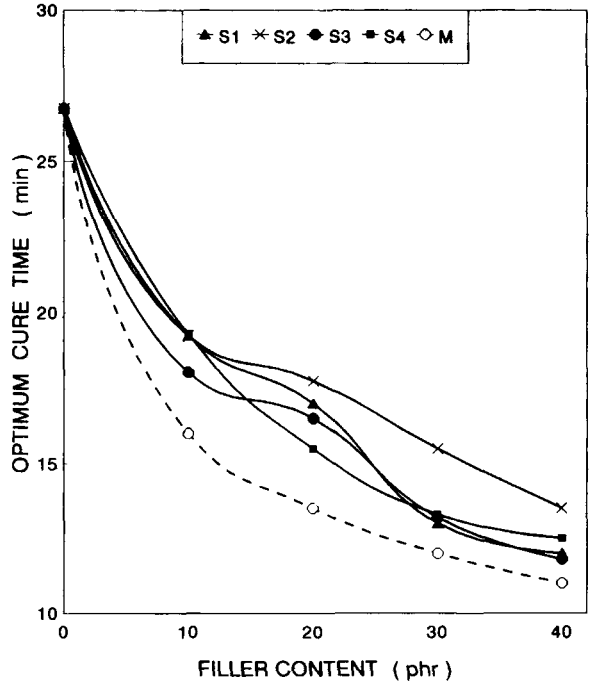

Figure 5 Variation of optimum cure time of SBR compounds with particle size and loading of filler.

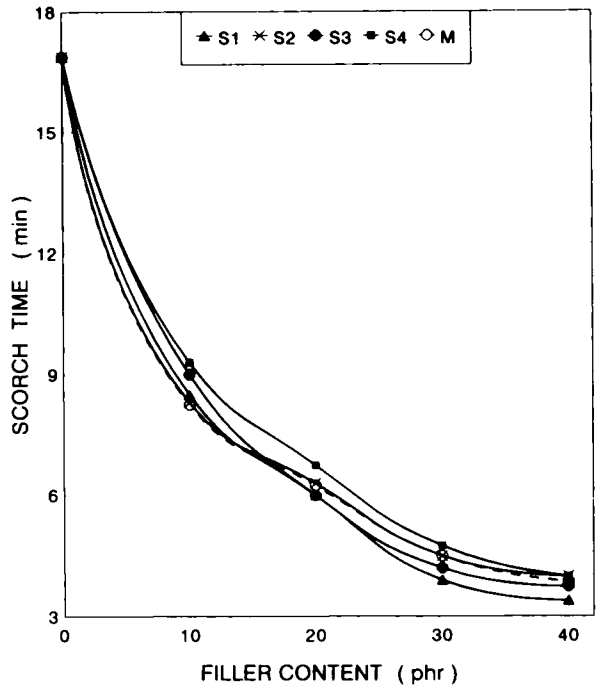

Figure 6 Variation of scorch time of SBR compounds with particle size and loading of filler.

Processing Characteristics

The processing characteristics of the blends are shown in Figures 5–9. The variation of optimum cure time (time for attaining 90% of the maximum torque), scorch time (premature vulcanization time), and induction time (time needed to start vulcanization) are presented in Figures 5, 6, and 7, respectively. A considerable decrease in all these three parameters is noted with increasing loading of filler in SBR. This is due to the presence of unreacted curatives in the latex rejects. Prophylactics, as well as gloves, are manufactured by a latex dipping process, which needs a very fast accelerator. The accelerator used by the company is ZDEC, i.e., zinc diethyl carbamate having the structure:

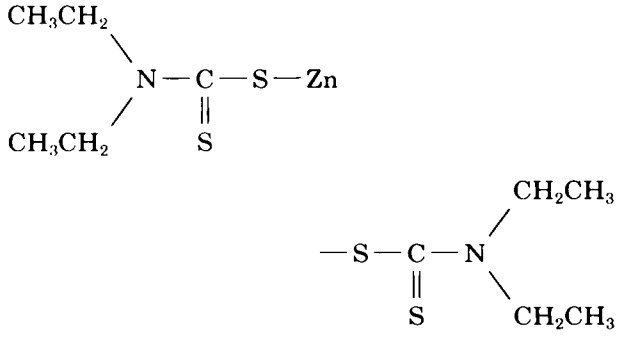

Some of this accelerator will remain unreacted after the curing process. This is extracted using spectroscopic grade acetone, and the spectrum of the dry sample is given in Figure 8. The peak at 790–770 cm^{-1} indicates the presence of ethyl chain ($-CH_2CH_3$), and that at 700–600 cm^{-1} is due to $C-S_{str}$. The $C=S_{str}$ is clearly visible at the 1250–1020 cm^{-1} range, and the peak at 2820–2760 cm^{-1} confirms the presence of $N-CH_2$ group in the compound. This observation indicates the presence of unreacted accelerator in the NR prophylactics. As the loading of NR prophylactics increases, the availability of the unreacted accelerator also increases, which leads to further reduction in curing characteristics, such as optimum cure time, scorch time, and induction time. The decrease in optimum cure time is minimum for SBR filled with size 2 filler and maximum for SBR loaded with mill sheeted form. The reduction in scorch time as well as induction time is maximum for SBR filled with size 1 filler and minimum for that with size 4 filler.

The general equation for the kinetics of a first-order chemical reaction can be written as

$$\ln(a - x) = -kt + \ln a \qquad (1)$$

where a = initial reactant concentration, x = reacted quantity of reactant at time t, and k = first-order

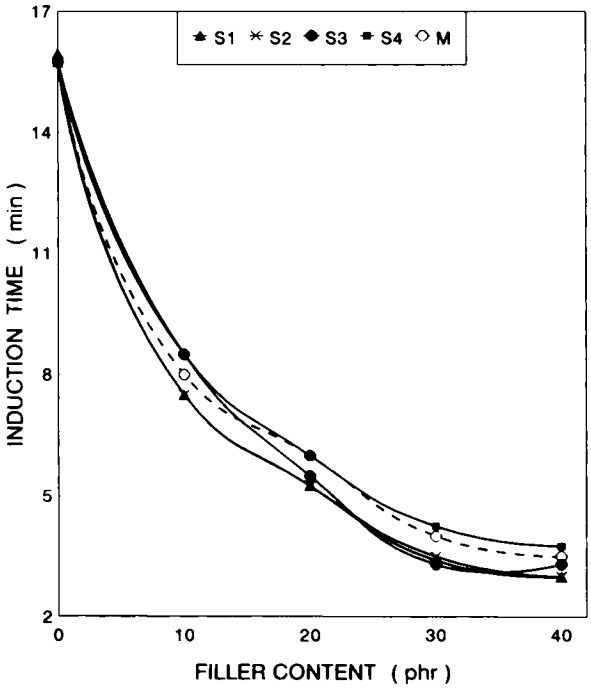

Figure 7 Variation of induction time of SBR compounds with particle size and loading of filler.

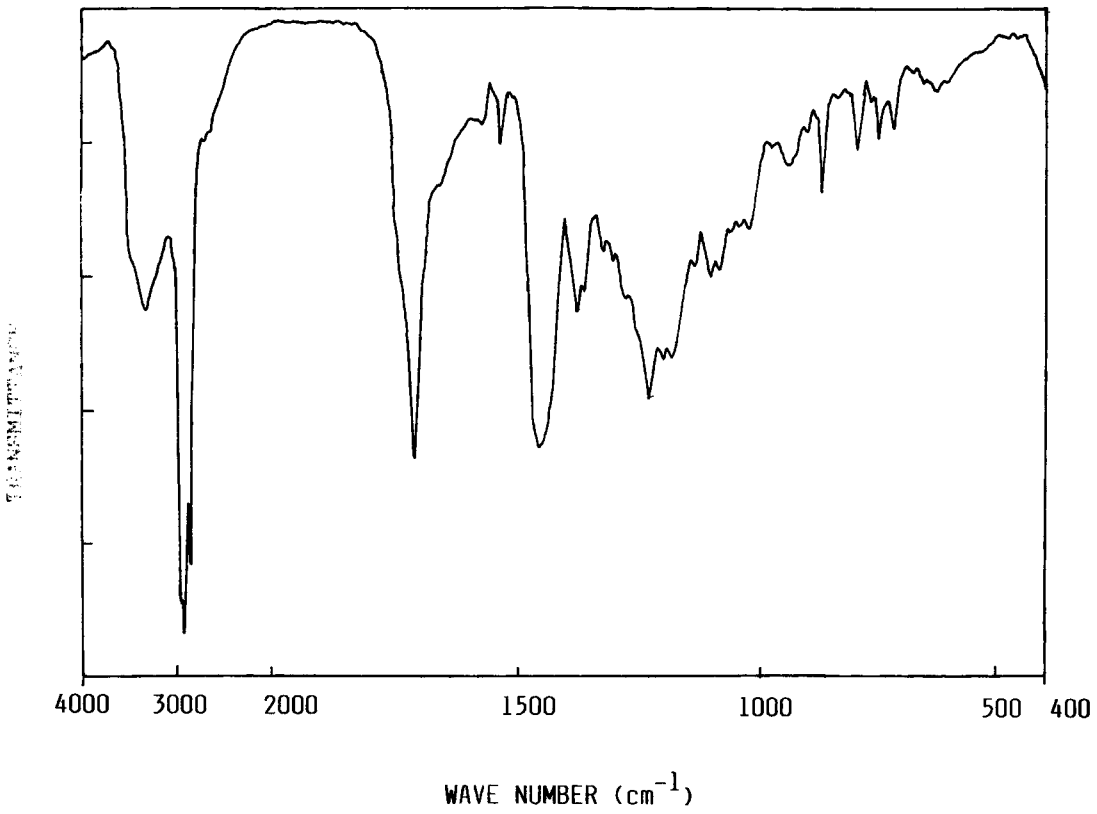

Figure 8 IR spectrum of the unreacted accelerator (ZDEC).

reaction rate constant. For the vulcanization reaction of rubber, the rate of crosslink formation is usually monitored by measuring the torque developed during vulcanization. The torque values so obtained are proportional to the modulus of the rubber. So if the change in a physical property such as modulus is measured, rather than the change in reactant concentration, the following substitutions can be made.

$$(a - x) = (M_\infty - M) \tag{2}$$

$$a = M_\infty - M_o \tag{3}$$

where M_∞ is the maximum modulus, M_o is the minimum modulus, M is the modulus at time t. Substituting torque values for modulus, we get

$$(a - x) = (M_h - M_t) \quad \text{and} \quad a = M_h - M_o \tag{4}$$

where M_h is the maximum torque, M_o is the minimum torque and, M_t is the torque at time t. When $\ln(M_h - M_t)$ is plotted against t, a straight line graph is obtained as shown in Figure 9, which proves that the cure reaction of the gum and filled SBR compound follows first-order kinetics. The cure reaction rate constant (k) values are obtained from the slope of the straight lines. These values are presented in Table III. The rate constant values generally increase with increasing filler loading. The higher the loading, the greater the amount of curatives available. This indicates an increase in the rate of crosslinking. This increase of rate constant is most noted for SBR loaded with mill sheeted form of the filler.

Figure 10 represents the variation of Wallace plasticity (100°C) with increasing loading of filler. Since Wallace plasticity is a direct measure of the elastic recovery of the rubber compound, its increase with increasing filler loading is extremely advantageous as far as rubber compound is concerned. The Wallace plasticity at 40 phr filler loading is found to be minimum for SBR loaded with mill sheeted form of the filler.

Mechanical Properties

Figure 11 represents the stress–strain curves of the gum and filled (size 1 filler) SBR compounds. The stress–strain behavior of filled SBR vulcanizate is

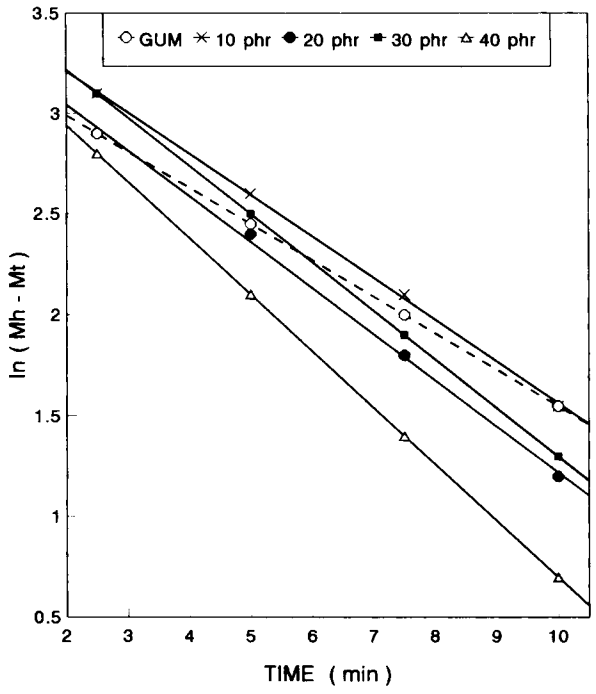

Figure 9 Plots of $\ln(Mh - Mt)$ versus time (min) of gum and filled (size 1) SBR compounds.

controlled by the characteristics of the filler and the matrix. The deformation behavior seen from the curves is almost similar for gum and filled samples. At higher strains, the stress value is found to be increasing slowly, rather than exhibiting yielding behavior. This behavior is typical of vulcanized low strength materials. The elongation at break exhibits a good increase with increasing filler loading (Fig. 12). At higher loadings of the filler, this increase is predominant for SBR vulcanizates filled with size 2, 3, and 4 fillers, while size 1 shows lower values. Mill sheeted form stands midway between these two extremes. The observed increase in elongation at break with increasing filler loading may be due to the ability of NR latex waste filler particles to elongate to high strains. The decrease in crosslink density with increasing filler loading also contributes to the increase in elongation at break values. The crosslink density values are given in the following section. The Young's modulus values are shown in Table III. They are found to be unaffected at lower loadings of the filler, while a slight decrease is observed at higher loadings for most of the cases. The modulus at 300% elongation (M-300) presented in Table III decreases up to 30 phr and then increases slightly for 40 phr filler loading. The above said abnormal nature of moduli values may be due to two opposing factors, namely, crosslink density reduction and reinforcement, with increasing loading of the filler. When reduction in crosslink density with filler loading tends to decrease the modulus, the reinforcement by the filler tends to increase it. These factors compete with each other. Therefore, the observed behavior is the net effect of these two factors.

A remarkable increase in tensile strength is observed with increasing filler loading as shown in Figure 13. This points out the fact that latex waste filler has some reinforcing effect in SBR matrix. This reinforcing effect observed with increasing loading of NR prophylactics is due to the strain crystallization behavior of crosslinked NR latex filler. In a weak matrix like SBR, NR latex filler is found to retain its strain crystallizing nature, even if it is in the form of a fine filler. But contrary to the usual behavior of fine filler (size 1) being more reinforcing, here, the largest size (size 4) and mill sheeted form show relatively good tensile properties. This is due to the sulfur diffusion phenomena noted here and reported earlier in similar systems.[24] For the fine filler (size 1), the contact surface area with the SBR matrix is more. This can lead to an increase in sulfur migration from the matrix to the filler phase. Enhanced sulfur migration weakens crosslinks in the matrix, so the tensile properties which were expected to be superior for size 1 filler actually become inferior. The extent of sulfur migration is controlled not only by the particle size of the filler but also by the degree of polysulfidic linkages in the filler. The degree of polysulfidic linkages in the filler has a direct relation with the extent of sulfur migration.[15] Mill sheeted form of the latex waste filler is prepared by passing the waste through a two-roll mill for 10 min. This leads to substantial breakdown of the polysulfidic linkages resulting in a low degree of polysulfidity for mill sheeted form.[15] It is obvious that mill sheeted form also undergoes size reduction during the mixing procedure. Still the extent of sulfur diffusion is least in SBR compounds filled with mill sheeted form. Owing to this, they show better values of tensile strength over others.

The tear strength of SBR compounds (Fig. 14) also show an increase with increasing loading of filler. The particles of NR latex waste filler present in the tear path elongate to high strains and obstruct tear front. Among the filler sizes used, smaller sizes S_1, S_2, and S_3 show the maximum tear strength at 40 phr loading. Size 4 filler is inferior to these both at low and high filler loading. For SBR compounds containing fillers of smaller sizes, there will be a large number of filler particles present per unit area to elongate to high strains and to obstruct the advancing tear. As far as tear strength is concerned,

Table III Rate Constant and Modulus Values

SBR Compound	Cure Reaction Rate Constant (k) (sec^{-1})	Young's Modulus (MPa)	$M - 300$ (MPa)
Gum SBR	0.18	1	0.92
Size 1 Filler			
10 phr	0.21	1	0.91
20 phr	0.22	1	0.88
30 phr	0.24	1	0.90
40 phr	0.28	0.77	0.97
Size 2 Filler			
10 phr	0.23	1	0.92
20 phr	0.29	1	0.79
30 phr	0.24	1	0.79
40 phr	0.25	1	0.86
Size 3 Filler			
10 phr	0.24	1	0.91
20 phr	0.25	1	0.88
30 phr	0.24	1	0.86
40 phr	0.34	0.85	0.95
Size 4 Filler			
10 phr	0.20	1	0.79
20 phr	0.26	0.80	0.78
30 phr	0.23	0.80	0.86
40 phr	0.30	0.70	0.70
Mill Sheeted Filler			
10 phr	0.36	1	0.94
20 phr	0.37	0.85	0.92
30 phr	0.33	0.80	0.87
40 phr	0.42	0.80	0.95

the performance of compounds containing fillers of smaller particle sizes is superior to others. The effects of filler loading on IRHD hardness are shown in Figure 15. The observed decrease in IRHD hardness with increasing filler loading is due to the decrease in crosslink density.

Swelling Studies and Crosslink Density Determination

Swelling index values represent the swelling resistance of rubber compound and are calculated using the equation

$$\text{Swelling index } \% = \frac{W_2 - W_1}{W_1} \times 100 \qquad (5)$$

where W_1 is the initial weight of the circular specimen cut from the cured rubber slabs, and W_2 is the final weight of the specimen (after equilibrium swelling in toluene). The swelling index values are shown in Table IV. The value obtained for the gum SBR compound is lower than that of any other filled system. This indicates that the gum compound has more resistance to swelling than the filled SBR compounds. This observation points to the decrease in crosslink density in filled compounds, which again, is a consequence of sulfur migration. With increasing filler loading, swelling index values are found to be increasing, but the increase is not always uniform. For a fixed filler loading, the value is minimum for the SBR compound filled with the mill sheeted form of the filler. This indicates comparatively better reinforcement in SBR vulcanizates loaded with mill sheeted form of the filler. The crosslink density ($1/2Mc$) was determined using the following Flory–Rehner equation

$$Mc = \frac{-\rho_r V^s (V^{rf})^{1/3}}{\ln(1 - V^{rf}) + V^{rf} + \chi V^{rf2}} \qquad (6)$$

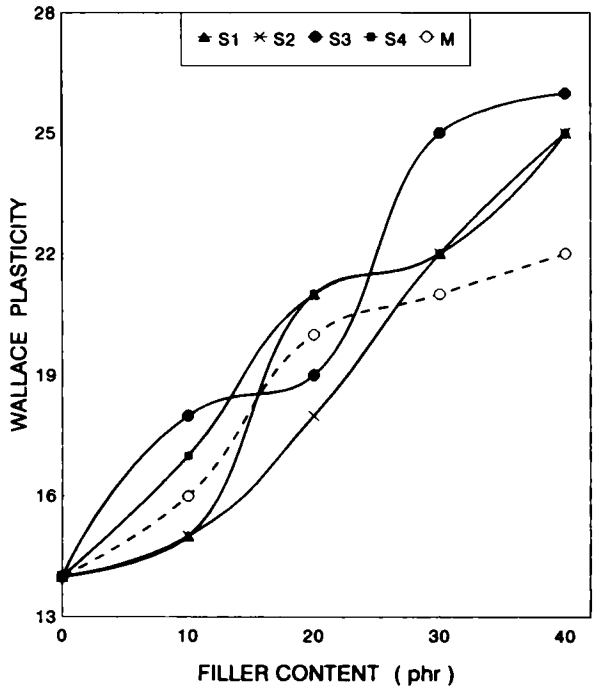

Figure 10 Variation of Wallace plasticity of SBR compounds with particle size and loading of filler.

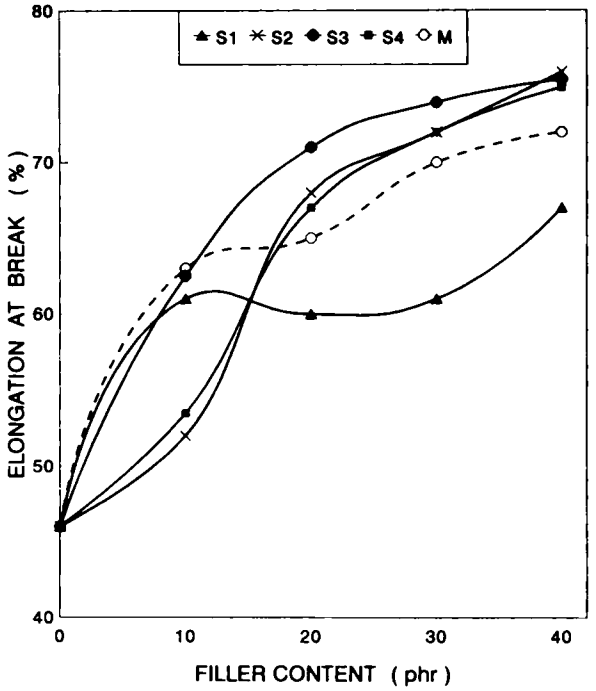

Figure 12 Effect of the size and loading of filler on the elongation at break of SBR vulcanizates.

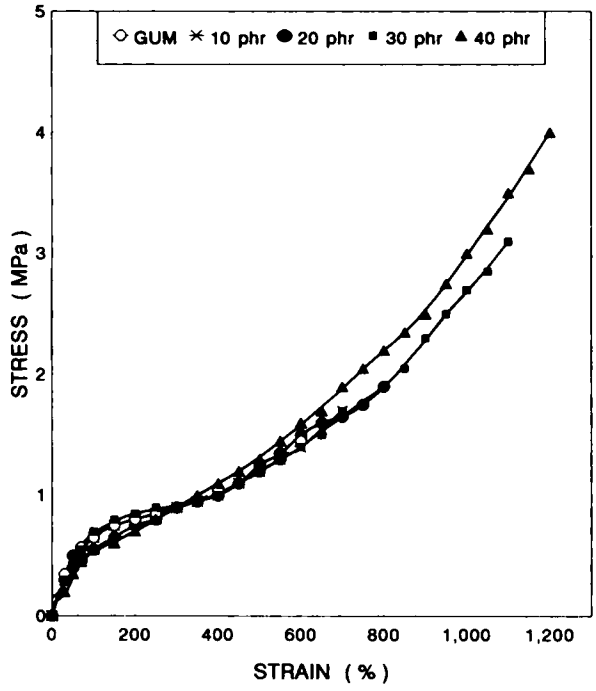

Figure 11 Stress–strain curves of gum and filled (size 1) SBR vulcanizates.

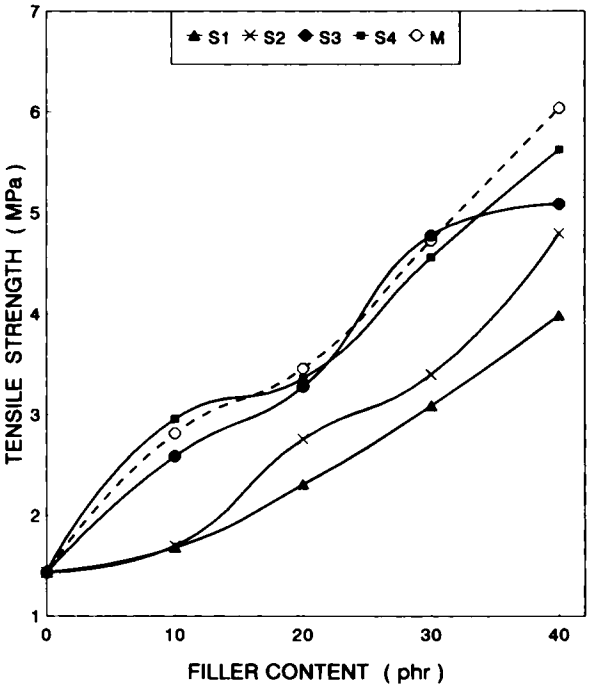

Figure 13 Effect of the size and loading of filler on the tensile strength of SBR vulcanizates.

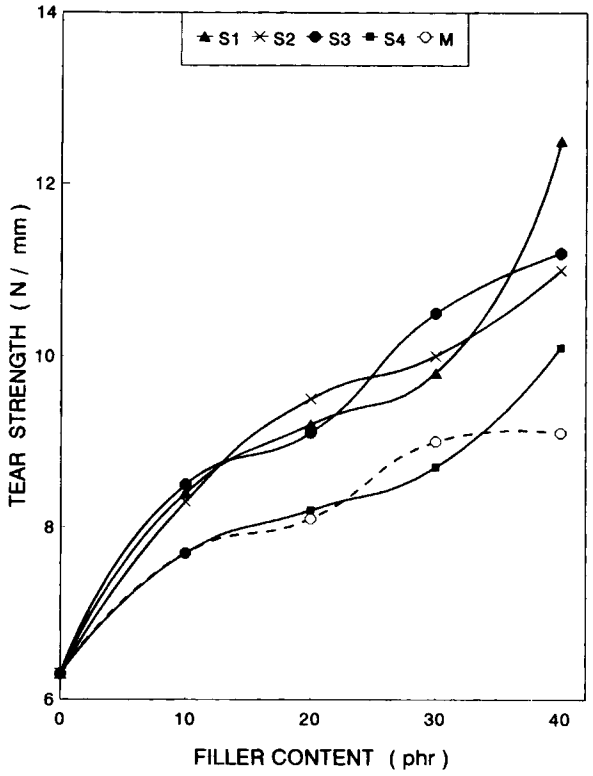

Figure 14 Effect of the size and loading of filler on the tear strength of SBR vulcanizates.

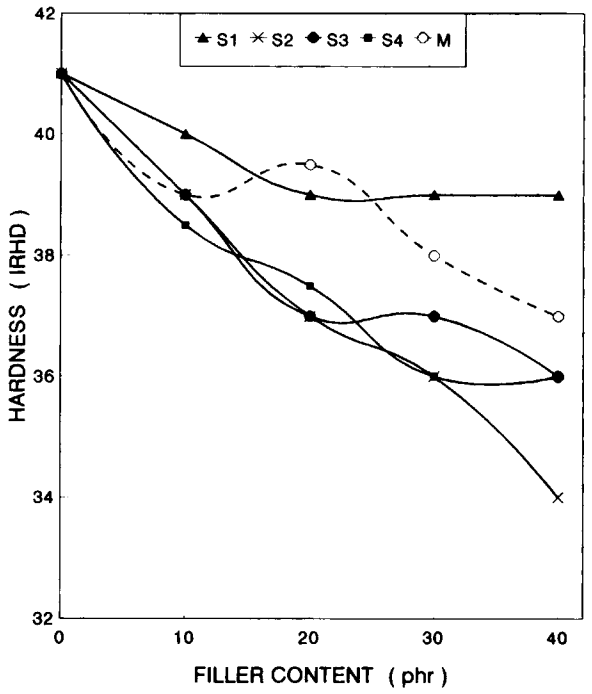

Figure 15 Effect of the size and loading of filler on the hardness (IRDH) of SBR vulcanizates.

where ρ^r is the density of the polymer; V^s, the molar volume of the solvent; V^{rf}, the volume fraction of elastomer in solvent swollen filled samples; and χ, the interaction parameter, which is given by the equation

$$\chi = \beta + (V^s/RT)(\delta^s - \delta^p)^2 \quad (7)$$

where β is the lattice constant; R, the universal gas constant; T, the absolute temperature; δ^s is the solubility parameter of the solvent; and δ^p, the solubility parameter of the polymer.

The variation of crosslink density as a function of increasing filler loading is given in Figure 16. As a result of sulfur migration from the SBR matrix to the filler phase, the crosslink density of the matrix phase decreases. This can lead to a decrease in the swelling resistance of filled systems. This crosslink density decrease is minimum for SBR vulcanizates containing mill sheeted form of the filler. This is due to the lower degree of polysulfidic linkages in the mill sheeted form, which always retards sulfur migration.[15] For SBR vulcanizates loaded with fillers of smaller particle sizes, enhanced sulfur diffusion causes much reduction in crosslink density.

Extent of Reinforcement

The extent of reinforcement is assessed by using Kraus and Cunneen and Russel equations.

According to Kraus equation,[29]

$$V^{ro}/V^{rf} = 1 - m\left[\frac{f}{1-f}\right] \quad (8)$$

where V^{rf} is the volume fraction of rubber in the solvent swollen filled sample and is given by the equation

Table IV Effect of the Size and Loading of Filler on the Swelling Index Value of SBR Compounds

	Swelling Index Values (%) Filler Loading (phr)				
Sample	0	10	20	30	40
Gum	427				
Size 1		439	469	503	463
Size 2		447	489	520	526
Size 3		461	497	485	497
Size 4		462	476	477	468
M		431	428	449	449

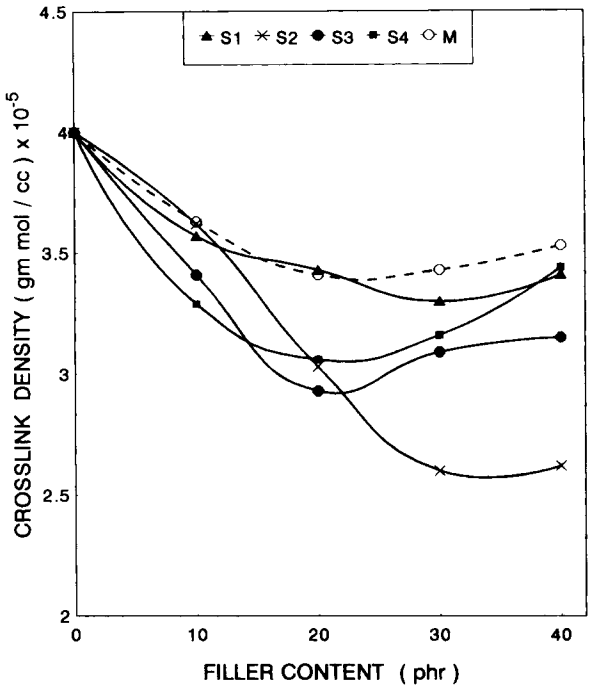

Figure 16 Variation of crosslink density of SBR vulcanizates with particle size and loading of filler.

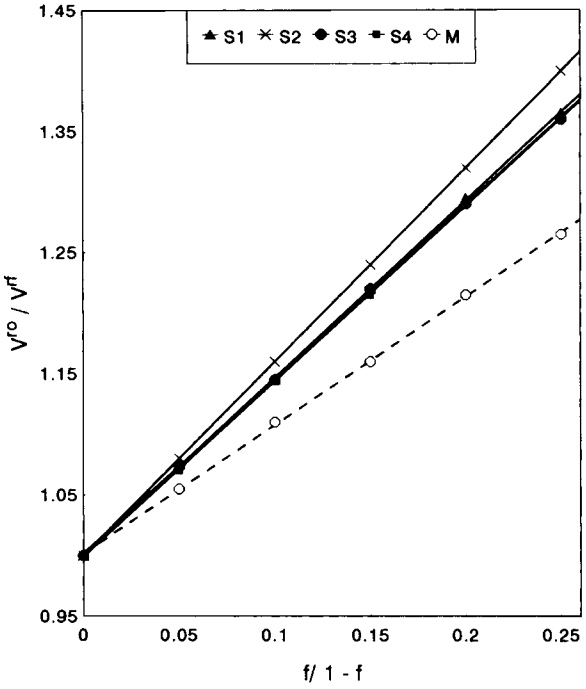

Figure 17 Plots of $\frac{V^{ro}}{V^{rf}}$ vs. $\frac{f}{1-f}$ of SBR vulcanizates.

$$V^{rf} = \frac{(d - fw)\rho_p^{-1}}{(d - fw)\rho_p^{-1} + A^s\rho_s^{-1}} \tag{9}$$

where d is the deswollen weight of the sample; f, the volume fraction of the filler; w, the initial weight of the sample; ρ_p, the density of the polymer; ρ_s, the density of the solvent; and A^s, the amount of solvent absorbed. For an unfilled system, $f = 0$. If we substitute $f = 0$ in eq. (9), we get the expression for the volume fraction of rubber in the solvent swollen unfilled sample (V^{ro}).

$$V^{ro} = \frac{d\rho_p^{-1}}{d\rho_p^{-1} + A^s\rho_s^{-1}} \tag{10}$$

Since eq. (8) has the general form of an equation for a straight line, a plot of V^{ro}/V^{rf} as a function of $f/1 - f$ should give a straight line, whose slope (m) will be a direct measure of the reinforcing ability of the filler used. The more the reinforcing ability of the filler, the more will be the swelling resistance caused by that filler. A constant C, which is characteristic of the filler, is also calculated using the equation

$$C = \frac{m - V^{ro} + 1}{3(1 - V^{ro1/3})} \tag{11}$$

where m is simply the slope of the line plotted, according to eq. (8). The plots of Kraus equation for various particle sizes of fillers are shown in Figure 17, and the values of slopes and C are presented in Table V. According to the theory developed by Kraus[29] for highly reinforcing carbon blacks, negative higher slope values indicate a better reinforcing effect. In the present study, we observed that as the filler loading increases, the amount of solvent absorbed (A^s) also increases considerably. This increase will cause a reduction in the V^{rf} value calculated using eq. (9). Since V^{ro} remains unaffected with filler loading, the ratio V^{ro}/V^{rf} increases considerably with the increasing loading of filler, which gives rise to a positive slope. It is clear from Figure

Table V Values of Slopes and C

	Kraus Equation		Cunneen and Russell Equation
Particle Size	Slope (m)	C	Slope (a)
S1	1.46	1.67	2.8
S2	1.6	1.77	3.3
S3	1.43	1.64	1.9
S4	1.43	1.64	1.3
M	1.1	1.41	1

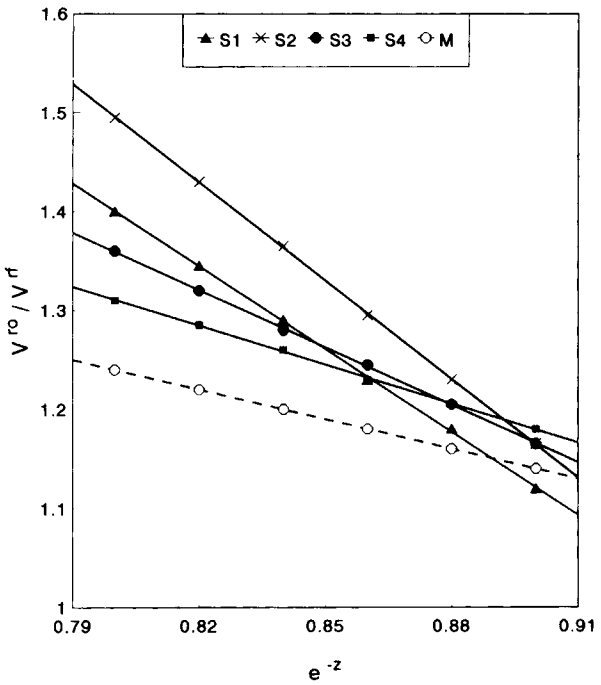

Figure 18 Plots of V^{ro}/V^{rf} vs. e^{-z} of SBR vulcanizates.

17 that the slopes are positive and are higher for SBR loaded with smaller sized fillers. The slope is found to be the lowest for SBR filled with mill sheeted form. So it is clear that SBR vulcanizate containing the mill sheeted form of the filler absorb a minimum amount of solvent. Therefore, the decrease in V^{rf} is comparatively less; hence, the ratio V^{ro}/V^{rf} is the least at a particular loading. This compound therefore presents a lower positive slope compared to others. This suggests that as far as the extent of reinforcement is concerned, the mill sheeted form is superior to other fillers.

The Cunneen and Russell equation[30] is given by

$$V^{ro}/V^{rf} = ae^{-z} + b \qquad (12)$$

V^{ro} and V^{rf} has the same meaning as explained above, and z is the weight fraction of the filler used. A plot of V^{ro}/V^{rf} versus e^{-z} should give a straight line whose slope, a, will be directly proportional to the reinforcing ability of the filler. The plots of the Cunneen and Russell equation are shown in Figure 18, and the slope a values are presented in Table V. In this case, V^{ro}/V^{rf} also increases with increasing filler loading, and this increase is most noted for fillers of smaller particle sizes. Comparatively highly reinforcing mill sheeted form of the filler absorb minimum amount of solvent. Therefore, the SBR vulcanizate loaded with the mill sheeted form of the filler shows the lowest V^{ro}/V^{rf} value at a particular loading and presents a smaller positive slope. Both Kraus and Cunneen and Russell equations point out the comparatively higher reinforcing nature of the SBR vulcanizates containing the mill sheeted form of the filler.

Three Layer Model for Sulfur Diffusion Experiment

The diffusion of sulfur from the SBR matrix to the filler phase is analyzed by using a three layer model,[24] as shown in Figure 1. The dimensions of the model are also given. The crosslink density of the sample obtained from the contact area of the middle latex waste layer is found to be higher than that of the sample obtained from the noncontact area. This is clear from Table VI. The same trend is reflected in the swelling index values presented in the same table. This is because of the sulfur diffusion from the outer gum SBR layers to the middle latex waste layer. This sulfur diffusion causes an increase in the crosslink density of the middle layer at the area in contact with outer SBR layers. At the area of the middle latex waste layer, which is separated from the outer gum SBR layers by the aluminium foil, sulfur diffusion cannot occur, so the crosslink density values here are found to be comparatively lower.

Morphology and Fractography

The tensile as well as tear strengths of the polymers are related to the morphological features of the fracture surface. Figures 19–23 represent the SEM pictures of tensile and tear fractured surfaces. In all the figures, it is possible to see the filler particles as phase separated entities, and this observation confirms the noncompatible nature of these filled samples; so these systems can be considered only as a natural rubber prophylactics filled SBR composite, not a true compatible blend of NR and SBR. It can also be seen from these figures that latex waste particles have undergone size reduction during mixing. The SEM of the failed tensile gum vulcanizate is presented in Figure 19(a). Here, the fracture is

Table VI Swelling Index and Crosslink Density Values From Sulfur Diffusion Experiment

Sample	Swelling Index (%)	Crosslink Density (g mol/cc) $\times 10^{-5}$
CS	427	2.75
NCS	576	1.65

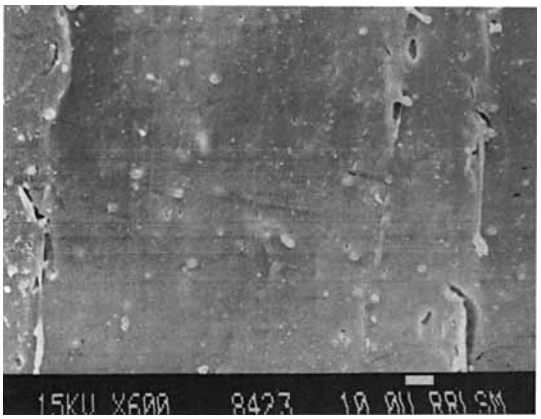

(a)

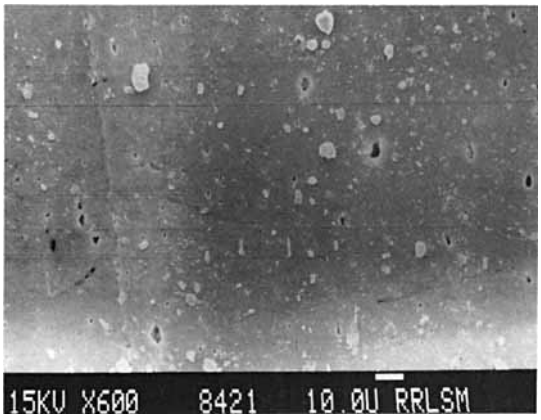

(b)

Figure 19 SEM photographs of the tensile fractured surface of gum SBR vulcanizate (a) and the tear fractured surface of gum SBR vulcanizate (b).

smooth without any deviation. This observation is in agreement with the low tensile strength of the gum SBR vulcanizate. The SEM of the failed tear gum vulcanizate, shown in Figure 19(b), also presents smooth torn areas. This indicates its low tear properties.

The tensile fractured surface of filled (40 phr of size 1) SBR vulcanizate are presented in Figure 20(a). Here, the fracture is not smooth as in the case of gum. As a result of enhanced sulfur migration, dewetting is observed in this case, as shown in Figure 20(b).

Figure 21(a) represents the torn surface of the SBR vulcanizate filled with 40 phr of size 1 filler. The figure shows crack deviation due to the restriction to crack propagation by filler particles. In this case also, dewetting is observed, as can be seen from Figure 21(b). The observation of dewetting is in agreement with the noncompatibility behavior of these filled systems discussed earlier.

The tensile and tear fractured surface of SBR vulcanizate loaded with 40 phr (size 4) filler is shown in Figures 22(a) and (b), respectively. In both cases, extensive crack deviation can be seen.

Figure 23(a) is the tensile fractured surface of the SBR vulcanizate filled with the 40 phr mill sheeted

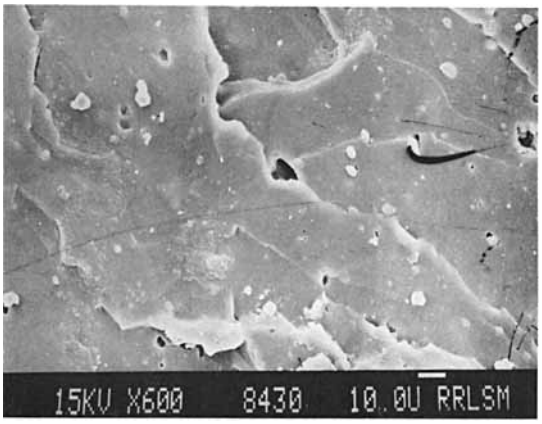

(a)

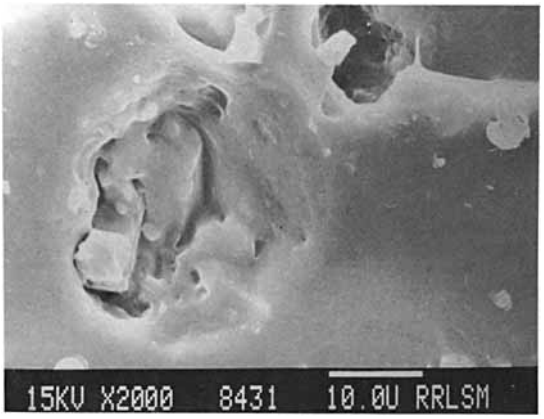

(b)

Figure 20 SEM photographs (a) and (b) of the tensile fractured surface of filled (size 1) SBR vulcanizate.

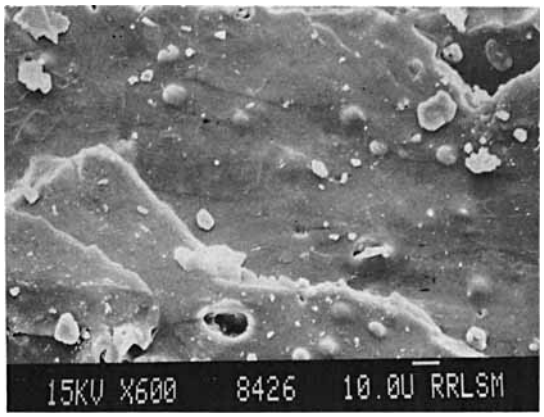

(a)

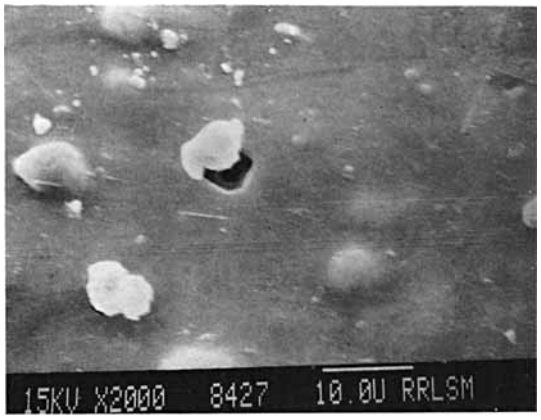

(b)

Figure 21 SEM photographs (a) and (b) of the tear fractured surface of filled (size 1) SBR vulcanizate.

form of the filler. Since sulfur diffusion is minimum in this case, filler–matrix adhesion is fairly good, and, hence, dewetting is less predominant. In this case also, filler particles obstruct the crack propagation and cause crack deviation. The torn surface of the SBR compound loaded with 40 phr of the mill sheeted form is presented in Figure 23(b). A sinusoidal wavy pattern at the fracture surface is a characteristic feature of high tear-resistant material.

In the case of all the filled compounds, torn surfaces show much crack deviation and present a series of parabolic tear lines distributed randomly. These parabolic tear lines result from the interaction of main fracture fronts with subsidiary fracture fronts and from the obstruction to tear propagation by filler particles. Reduced sulfur migration causes increase in filler–matrix adhesion in SBR vulcanizates filled with size 4 filler and mill sheeted form. The SEM pictures also indicate that the latex waste particles are not completely compatible with the SBR matrix. In all cases, the particles could be seen as phase separated entities.

CONCLUSION

The use of NR prophylactics waste as a potential filler in SBR is very attractive because of the sim-

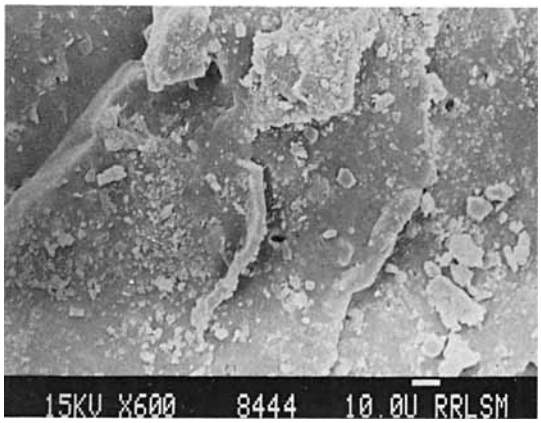

(a)

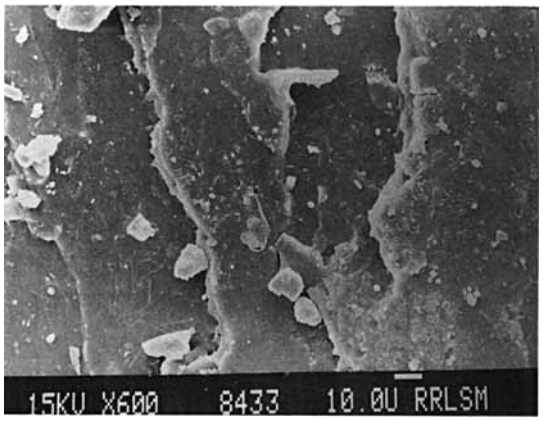

(b)

Figure 22 SEM photographs of tensile fractured surface of filled (size 4) SBR vulcanizate (a) and the tear fractured surface of filled (size 4) SBR vulcanizate (b).

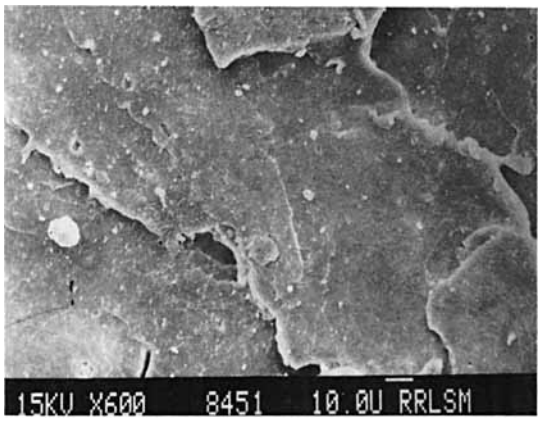

(a)

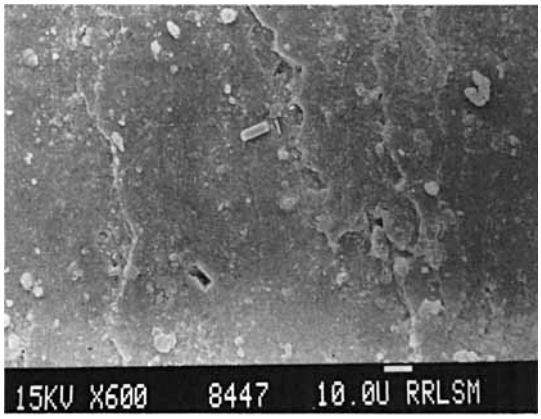

(b)

Figure 23 SEM photographs of the tensile fractured surface of filled (mill sheeted filler) SBR vulcanizate (a) and the tear fractured surface of filled (mill sheeted filler) SBR vulcanizate (b).

plicity of the latex waste grinding technique and the surplus nature of the NR prophylactics. NR latex waste has been ground into particles of various sizes. The particle size morphology and size distribution are analyzed. It has been noticed that with increasing filler loading, there is a reduction in optimum cure time, scorch time, and induction time and an increase in cure reaction rate constant. The Wallace plasticity, which is a measure of elastic recovery of rubber compound, increases with increasing filler loading. The above observations are advantageous as far as productivity and processability are concerned. Up to 40 phr filler loading, the tensile and tear properties show good improvement. The size 4 and mill sheeted form of the filler are found to exhibit superior tensile properties over others. The IRHD hardness values are found to be decreasing with increasing filler content. The swelling index values show a considerable increase, while the crosslink density shows a gradual reduction with increasing filler loading. The Kraus and Cunneen and Russell equations have been used to analyze the extent of reinforcement. These theories support the superior filler–matrix interaction in SBR vulcanizates loaded with the mill sheeted form of the filler. A three layer model has been developed to study the sulfur diffusion in filled SBR compounds. The results emanating from the sulfur diffusion experiment explain the reduction in crosslink density in filled SBR compounds. Compared to the production of fine rubber powder, the production of mill sheeted form of the filler is easy and economic. By wisely selecting the mill sheeted form of the filler, sulfur diffusion can be minimized, and the filler–matrix adhesion can be improved. The SEM examination of the tensile and tear fractured surfaces strongly supports the improved mechanical performance of the SBR vulcanizates filled with the mill sheeted form of the filler. The SEM studies also indicate that the crumb rubber particles are not completely compatible with the SBR matrix. Further studies are in progress to improve the adhesion of the rubber particles with the SBR matrix.

REFERENCES

1. A. A. Harshaft, *Environ. Sci. Technol.*, **6,** 412 (1972).
2. M. C. Kazarnowics, E. C. Osmundson, J. P. Boyle, and R. W. Savage, Paper presented at Rubber Div. Mtg., Am. Chem. Soc., Cleveland, Ohio, Oct 4–7, 1977; *Rubber Chem. Technol.* (abstr.), **51,** 386 (1978).
3. T. C. P. Lee and W. Millens, U.S. Patent 4,046,834 (1977) (to Gould Inc.).
4. L. E. Peterson, J. T. Moriarty, and W. C. Bryant, Paper presented at Rubber Div. Mtg., Am. Chem. Soc., Cleveland, Ohio, Oct. 4–7, 1977; *Rubber Chem. Technol.* (abstr.), **51,** 386 (1978).
5. N. R. Braton and J. A. Koutsky, *Chem. Eng. News.*, **52,** 21 (1974).
6. A. A. Phadke, A. K. Bhattacharya, S. K. Chakrabortthy, and S. K. De, *Rubber Chem. Technol.*, **56,** 726 (1983).
7. A. Ratcliffe, *Chem. Eng.*, **79,** 62 (1972).
8. M. W. Biddulph, *Conserv. Recycl.*, **1,** 169 (1977).
9. P. J. Zolin, N. B. Frable and J. F. Gentilcore, Paper presented at Rubber Div. Mtg., Am. Chem. Soc.,

Cleveland, Ohio, Oct 4–7, 1977; *Rubber Chem. Technol.* (abstr.), **51,** 385 (1978).
10. R. P. Burford and M. Pittolo, *Rubber Chem. Technol.*, **56,** 1233 (1983).
11. R. P. Burford, in *Energy Recovery and Utilization of Solid Wastes.* Nagoya, 1982, p. 507.
12. R. P. Burford and M. Pittolo, Talk 56, presented at Rubber Div. Mtg., Am. Chem. Soc., Philadelphia, 1982.
13. L. Slusarski and R. Sandlewski, *Int. Polym. Sci. Technol.*, **11,** 6 (1984).
14. K. Fujimoto and T. Nishi, *Int. Polym. Sci. Technol.*, **8,** 25 (1981).
15. K. Fujimoto, T. Nishi, and T. Okamoto, *Int. Polym. Sci. Technol.*, **8,** 30 (1981).
16. S. Yamashita, *Int. Polym. Sci. Technol.*, **8,** 77 (1981).
17. K. Fujimoto, T. Nishi, and T. Okamoto, *Int. Polym. Sci. Technol.*, **8,** 65 (1981).
18. S. V. Usachev et al., *Int. Polym. Sci. Technol.*, **12,** 30 (1985).
19. P. Elfferding, *Int. Polym. Sci. Technol.*, **9,** 30 (1982).
20. A. Acetta and J. M. Vergnaud, *Rubber Chem. Technol.*, **54,** 302 (1981).
21. A. Acetta and J. M. Vergnaud, *Rubber Chem. Technol.*, **55,** 961 (1982).
22. A. A. Phadke, S. K. Chakraborty, and S. K. De, *Rubber. Chem. Technol.*, **57,** 19 (1984).
23. A. A. Phadke and B. Kuriakose, *Kautschuk Gummi Kunststoffe*, **38,** 694 (1985).
24. L. N. Sharapova, A. A. Chekanova, N. D. Zakharov, and E. Yu. Borisova, *Int. Polym. Sci. Technol.*, **10,** 4 (1983).
25. Y. Onouchi, S. Inagaki, H. Okamoto, and J. Furukawa, *Nippon. Gomu. Kyokaishi*, **55,** 439 (1982).
26. N. M. Claramma, K. T. Thomas, and E. V. Thomas, Paper presented at the Rubber Conf., Jamshedpur, Nov. 6–8, 1986.
27. Y. Aziz, Paper presented at the Plastic Rubber Inst. Seminar, Aug. 4, 1990, Kuala Lumpur, Malaysia.
28. Y. Aziz, Paper presented at Polymer 90, Sept. 23, 1990, Kuala Lumpur, Malaysia.
29. G. Kraus, *J. Appl. Polym. Sci.*, **7,** 861 (1963).
30. J. I. Cunneen and R. M. Russell, *Rubber Chem. Technol.*, **43,** 1215 (1970).

Received July 10, 1995
Accepted April 5, 1996